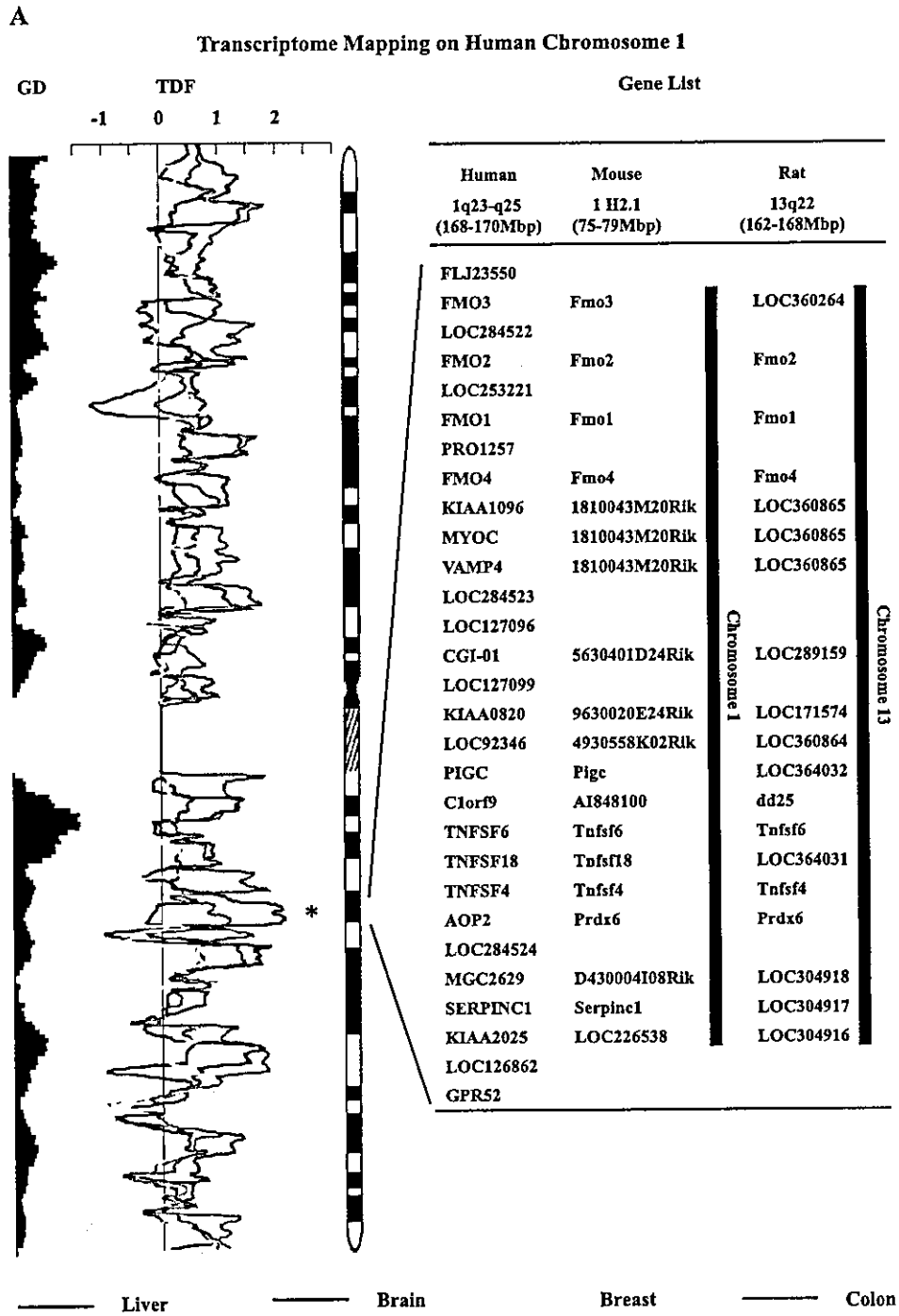

Fig. 2. Representative transcriptome map analysis of liver, brain, breast, and colon SAGE libraries. Differential expression patterns were observed in each tissue along the chromosome, and asterisks indicate the organ-related chromosomal domain. The genes located on the organ-related chromosomal domain in human are shown. Their possible homologous genes on mouse and rat genome are also shown.

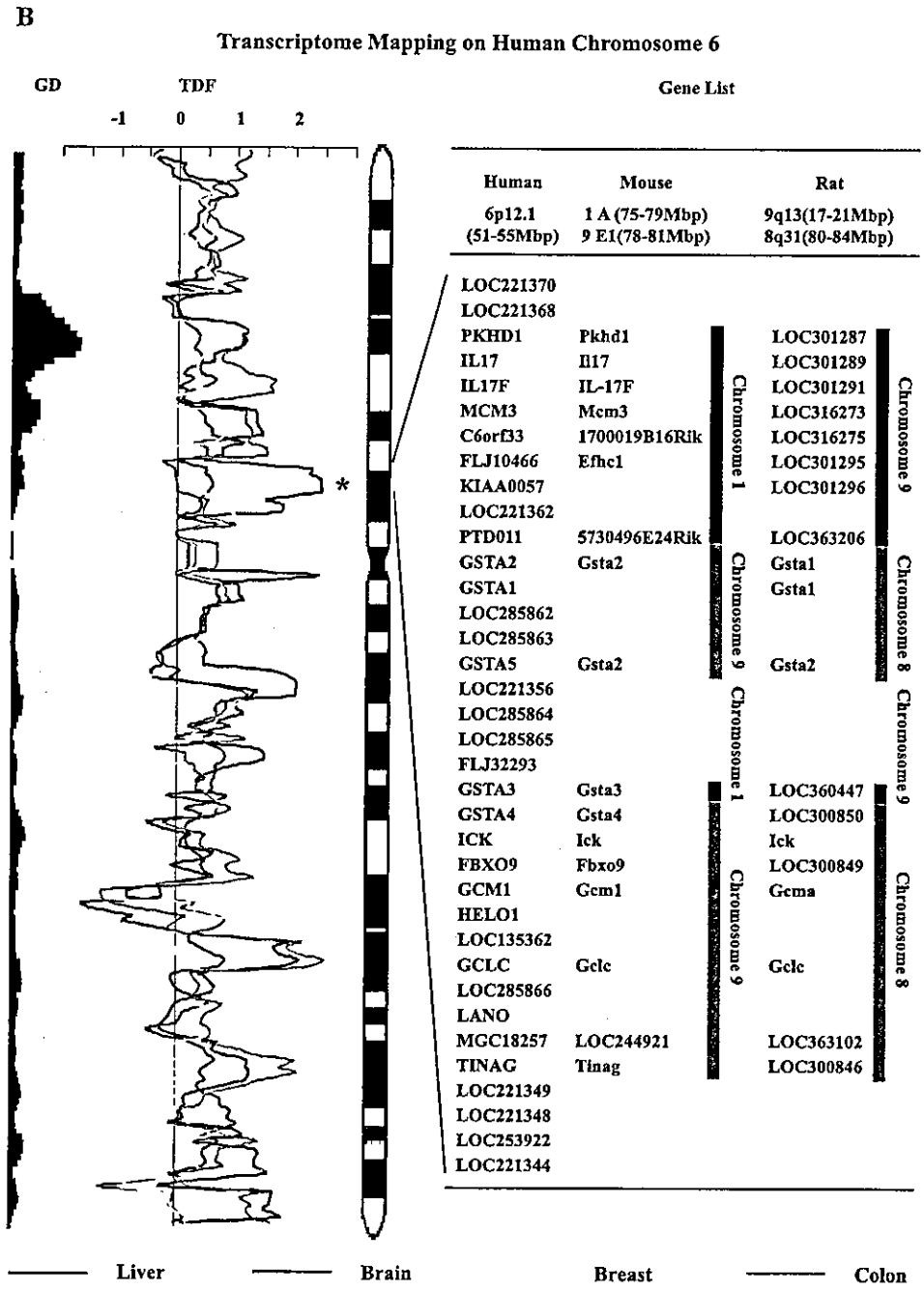

Fig. 2 (*continued*).

domains of the mouse and rat genomes (representative data of human 1q23–q25, mouse 1H2.1, and rat 13q22 are shown in Fig. 2). However, genes on chromosomes 6p12.1 and 21q22 were located on two different chromosomal domains of the rat and mouse genomes (representative data of human 6p12.1, mouse 1A and 9E1, and rat 9q13 and 8q31 are shown in Fig. 2). Interestingly, more than half of these chromosomal domains (1q23–q25, 4q21–q24, 6p12.1, 11q23, 18q12.1, and 21q22) contained multigene families. These data revealed that most of organ-related chromosomal domains identified here are conserved in the human and rodent genomes, which might have originated from chro-

Table 2
Cytogenetic loci of gene clusters highly expressed in each organ

Cytogenetic locus	Liver	Brain	Breast	Colon	Reference
Liver-related chromosomal domains					
1q23–q25	1,326	140	169	326	370
4q21–q25	2,104	132	139	129	352
6p12.1	983	189	166	84	210
11q23.1–q23.2	30,168	932	840	804	3552
17q11	3,329	777	445	385	778
18q12.1	1,752	26	26	28	168
Total	39,662	2196	1785	1756	5430
Colon-related chromosomal domains					
2p21	40	72	127	411	154
3q22–q23	59	55	86	406	116
8q13–q22.1	62	32	49	531	139
12q14.1–q21.1	35	37	53	510	132
21q22.3	25	52	100	1447	265
Total	221	248	415	3305	806

mosomal rearrangement and/or gene duplication during mammalian evolution (supplementary figure of all transcriptome mapping data and the gene list are available on our home page: http://www.intmedkanazawa.jp/).

Analysis of gene function on organ-related chromosomal domains

We investigated the functions of genes clustered on organ-related chromosomal domains using the Gene Ontology database (http://www.geneontology.org/). We could retrieve the information for 227 of 412 clustered genes from the Gene Ontology database, and 150 of these were annotated by molecular function. Interestingly, 74 of 150 genes were associated with metabolic enzymes, revealing that about half of the genes clustered on organ-related chromosomal domains are those encoding metabolic enzymes, suggesting the close relation of the chromosomal domains and some metabolic processes.

We searched the downstream targets of the genes on the organ-related chromosomal domains using PathwayAssist software and investigated the common targets and functions of the genes on the chromosomal domains. As shown in Table 3, 10 of 11 organ-related chromosomal domains consisted of genes associated with common metabolic or functional pathways, whereas no common targets were detected on chromosome 12q15 (colon-related chromosomal domain). Apparently, gene families associated with metabolism are clustered in liver-related chromosomal domains, such as 6p12.1 with xenobiotic metabolism, 4q21–q24 with alcohol and aldehyde metabolism, and 11q23–q24 with lipid metabolism. On the other hand, genes associated with transporters and apoptosis were clustered in colon-related chromosomal domains, such as 8q21 with anion transporter and 21q22 with apoptosis and cell proliferation. These data suggested that the genes clustered on organ-related chromosomal domains might be associated with the organ-specific functionality.

Discussion

The release of the sequence of the entire human genome and the development of advanced gene expression profiling technologies have focused interest on understanding the relationship between gene expression and chromosomal organization in complex systems. The genome is not simply a patchwork of genes but forms complex structures. The presence of chromosomal regions enriched in gene families has been demonstrated for several gene clusters. For example, the major histocompatibility complex is located on chromosome 6p21 [5], and the apolipoproteins are located on chromosome 11q23 [6]. It is not known, however, if genes abundantly expressed in each organ are distributed throughout the genome or clustered on various chromosomes. This question was addressed by assessing the chromosomal distribution of genes expressed in the brain and heart using EST collection databases [7,8]. Although these studies reported complex tissue-specific gene regulation patterns in the brain and heart, organ-specific gene expression patterns have not been compared simultaneously in several tissues. In addition, since EST databases are not generated according to the same methods by each distributor, comparison of the expression levels between organs may not be accurate. In this study, therefore, we utilized SAGE analysis to obtain unbiased gene expression data from hundreds of thousands of transcripts expressed in the normal human liver, brain, breast, and colon. Using genome-wide transcriptome maps for each organ, we identified six liver-related and five colon-related chromosomal domains. Thus, it seemed that organ-specific genes are accumulated on specific chromosomal domains for each organ.

Table 3
Functional annotation of the genes located on organ-related chromosomal domains

Cytogenetic locus	Function
Liver-related chromosomal domains	
1q23–q25	Xenobiotic mono-oxygenation; apoptosis and cell proliferation
4q21–q25	Alcohol and formaldehyde metabolism
6p12.1	Xenobiotic metabolism
11q23.1–q23.2	Lipid metabolism
17q11	Amyloid production
18q12.1	Focal contact; apoptosis and cell proliferation
Colon-related chromosomal domains	
2p21	Apoptosis and cell proliferation
3q22–q23	Ion transporter; apoptosis and cell proliferation
8q13–q22.1	Ion transporter; apoptosis and cell cycle regulation
12q14.1–q21.1	None
21q22.3	Apoptosis and cell proliferation; mucin production

Although the biological significance of this clustering of highly expressed, organ-related genes along the chromosomes is not clear, these clusters must provide significant advantages for tissue-specific functioning. The functional annotation of liver-related chromosomal domains revealed that they encoded metabolism-related genes such as for xenobiotic, lipid, and alcohol metabolism. The lipid and alcohol metabolism is liver specific. The functional annotation of colon-related chromosomal domains revealed that they encoded apoptosis, cell proliferation, ion transporter, and mucin production. These functions are essential for colon epithelium producing gut fluid and compatible with the short life span of the colon epithelium [9,10]. Thus, we first identified the presence of organ-related gene clusters in chromosomes and revealed their biological significance for organ-specific functioning.

In general, the relative proportions of cell types differ in each organ and affect the patterns of gene expression. In this study, we identified six liver-related and five colon-related chromosomal domains, whereas no brain-related or breast-related chromosomal domains were found on whole chromosome. It is possible that different compositions of cells might underestimate the presence of organ-related gene clusters in chromosomes.

What is the biological and evolutionary background of these organ-related chromosomal domains? In general, transcriptional machineries may access two coexpressed genes more efficiently when they are neighbors, so active transcription of organ-related chromosomal domains may result from the binding of a specific transcription factor to these domains [2]. Another possibility is that the formation of organ-related chromosomal domains in the human genome is the result of chromosome rearrangement during the process of evolution, because the organ-related chromosomal domains were conserved in one or two mouse and rat chromosomes. Recent comparative analyses of large-scale genome sequencing revealed that rearrangement of chromosomal segments and localized duplication of genomic segments are two major factors in eukaryotic genome evolution [11]. Our data revealed that half of the organ-related chromosomal domains contained multigene families. These results suggest that the gene duplications may also contribute to the formation of organ-specific functionality in mammalian evolution.

Recently, draft genome sequences of the Brown Norway rat were analyzed and compared with the human and mouse genomes, revealing that the human and rodent genomes contain conserved synteny blocks [12]. We therefore investigated the organ-related chromosomal domains with reported conserved synteny blocks in human, mouse, and rat genomes (http://www.genboree.org) and identified that all organ-related chromosomal domains were included in synteny blocks conserved in human and rodent genomes (data not shown). These data might indicate the proximity of the human and rodent genomes in mammalian evolution, and organ-related chromosomal domains may have constituted parts of synteny blocks of larger size during human, mouse, and rat genome evolution.

If the number of genes in a chromosomal domain were small and the transcriptional activity in most of a tissue were low in the 5-Mb window, we could not eliminate the effects of a single highly expressed gene on the TDF score. To eliminate this limitation, we set the region criteria of gene density to more than two genes in a window of 1 Mb. Another limitation of the method is the inability to reveal some chromosomal domains with equal up–down differential gene expression. Although the method in this study still has some limitations, our data could provide the candidate organ-related chromosomal domains and could highlight the neighboring genes on the domains with tissue specificity.

In conclusion, we have identified gene expression patterns along the chromosomes in normal human liver, brain, breast, and colon, showing the clustering of organ-related genes on specific chromosomal domains. Our results indicate that the human genome organization may be closely related to the organ-specific gene expression patterns.

Materials and methods

SAGE

To determine organ-specific gene expression patterns comprehensively along human chromosomes, we collected SAGE databases derived from normal tissues. To avoid individual variations in gene expression, we selected, for each tissue, SAGE libraries that contained at least 50,000 tags, and we used at least two libraries per tissue type. We analyzed publicly available SAGE libraries derived from normal brain (GSM676, GSM695), breast (GSM677, GSM780, GSM781), and colon (GSM728, GSM729) tissues (ftp://ftp.ncbi.nih.gov/pub/sage/). We also constructed SAGE libraries derived from normal liver tissues (http://www.intmedkanazawa.jp/) [13], as well as reference SAGE databases containing publicly available normal human brain, breast, colon, heart, kidney, liver, lung, prostate, and stomach SAGE libraries (GSM761, GSM677, GSM728, GSM1499, GSM708, GSM785, GSM762, GSM739, GSM739, and GSM784), each containing about 50,000 SAGE tags. All sequence files from these databases were analyzed with SAGE 2000 software, kindly donated by Drs. Kenneth W. Kinzler and Bert Vogelstein. The number of SAGE tags per library was normalized to 450,000 transcripts.

Transcriptome mapping

Gene identity and UniGene CLUSTER assignment of each SAGE tag were obtained from the SAGEmap reliable tag-to-gene mapping table (http://www.sagenet.org/SAGEDatabases/unigene.htm). Association of UniGene

clusters with chromosome positions was obtained from RefSeq build 31 (http://www.ncbi.nlm.nih.gov/RefSeq/) and LocusLink (http://www.ncbi.nlm.nih.gov/LocusLink/) databases (November 26, 2002). SAGE tag locations along the chromosomes were matched to physical distance information by connecting the SAGE map, RefSeq, and LocusLink tables with the UniGene number.

Transcription density and gene density

Transcriptional activity was determined from the TDF [7]. Briefly, TDF is calculated using a 5-Mb window moving along the chromosome at 1-Mb intervals and defined as $\mathrm{TDF} = \ln(R/R_{\mathrm{ref}})/(T/T_{\mathrm{ref}})$, where R is the number of SAGE tags in each library and T is the number of unique SAGE tags in each library, within a window of 5 Mb. Gene density is defined as the number of RefSeq records divided by the average RefSeq records in each 5-Mb window. The correlation between transcription density and gene density in each chromosome was assessed by calculating the Pearson's correlation coefficient using the equation

$$r = \frac{n\left(\sum_{i=1}^{n} XiYi\right) - \left(\sum_{i=1}^{n} Xi\right)\left(\sum_{i=1}^{n} Yi\right)}{\sqrt{\left\{n\sum_{i=1}^{n} Xi^2 - \left(\sum_{i=1}^{n} Xi\right)^2\right\}\left\{n\sum_{i=1}^{n} Yi^2 - \left(\sum_{i=1}^{n} Yi\right)^2\right\}}}$$

where X_i is the number of SAGE tags in each library and Y_i is the number of RefSeq records in each 5-Mb window.

To investigate the statistical significance of the TDF values selected, we performed a permutation test. The following argument explains a statistical method that tests the null hypothesis that two groups are equivalent in the distribution of orders of their members. The alternative hypothesis is that members of one of the groups tend to rank higher. By rejecting the null hypothesis, we show that selected members are significantly high-ranked in the order of a variable. First we set up the notation. Suppose that n regions are classified into two groups. Each region is indexed by i, where $i \in I := \{1,2,\ldots,n\}$ and I_1 denotes the set of indices of the first group of m regions. Assuming that an observed value x_i is attributed to the ith region, we denote the order statistics of the values by $x_{(1)} > x_{(2)} > \ldots > x_{(n)}$, where no tie is assumed to simplify the argument. Let a function $\rho(i)$, $i \in I$ uniquely assign to an index its rank: $x_i = x_{(\rho(i))}$.

A permutation test is adopted, and without loss of generality, we henceforth assume that $I_1 = \{1, 2, \ldots, m\}$. Under the null hypothesis,

$$Pr(\rho(1) = i_1, \rho(2) = i_2, \ldots, \rho(m) = i_m) = \frac{1}{\binom{n}{m}}$$

for all the elements of $\{(i_1, i_2, \ldots i_m) \in I^m \mid \forall j \neq k\, i_j \neq i_k\, (j,k) \in I_1^2\}$.

Let us consider the test statistic $T = \sum_{i=1}^{m} \rho(i)$ where the null hypothesis is rejected for some c if $T < c$. Consequently, the p value of a realized test statistic t is given by $Pr(T \leq t)$. In particular, if the regions of the first group are ranked from the first to the mth, the p value reduces to

$$Pr\left(T \leq \frac{m(1+m)}{2}\right) = \frac{1}{\binom{n}{m}}$$

To be concrete, let us regard x_i as the TDF of the ith region, for example. Top m ranks group together under the criterion that selects the regions where TDFs are larger than 1.8. Hence its significance is easy to evaluate by the aforesaid method, and the rejection of the null hypothesis implies that the selected regions' TDFs are larger. Similarly, if we select the regions where an objective organ's TDF is larger than 1.8 and other organs' TDFs are smaller than 1.0, just regard x_i as the number of organs whose TDFs are smaller than 1.0. Then top m ranks consist of the selected regions among n regions where an objective organ's TDF is larger than 1.8. In this case, the rejection of the null hypothesis implies that the TDFs of organs other than the objective are relatively small in the selected regions.

Comparison of organ-related chromosomal domains in rat, mouse, and human genomes

All genes located on organ-related chromosomal domains in human were listed using the RefSeq build 31 database (http://www.ncbi.nlm.nih.gov/RefSeq/). All possible homologous genes and their locations on the *R. norvegicus* and *M. musculus* genomes were searched using the HomoloGene database (February 20, 2004) (http://www.ncbi.nlm.nih.gov/entrez/query.fcgi?DB=homologene). The chromosomal location and the gene list on each domain were also confirmed by MapViewer (http://www.ncbi.nlm.nih.gov/mapview/).

Pathway analysis

To investigate the functions of genes located on organ-related chromosomal domains comprehensively, we used PathwayAssist software (Ariadone Genomics, Rockville, MD, USA). All genes located on the chromosomal domains were investigated and annotated with the biological processes, protein–protein interactions, and gene regulatory networks using a reference-based data file.

Acknowledgment

The authors thank Dr. Koichi Miwa for providing human liver tissues.

References

[1] H. Caron, et al., The human transcriptome map: clustering of highly expressed genes in chromosomal domains, Science 291 (2001) 1289–1292.
[2] P.J. Roy, J.M. Stuart, J. Lund, S.K. Kim, Chromosomal clustering of muscle-expressed genes in Caenorhabditis elegans, Nature 418 (2002) 975–979.
[3] P.T. Spellman, G.M. Rubin, Evidence for large domains of similarly expressed genes in the Drosophila genome, J. Biol. 1 (2002) 5.
[4] G.M. Rubin, et al., Comparative genomics of the eukaryotes, Science 287 (2000) 2204–2215.
[5] H. Abderrahim, et al., Cloning the human major histocompatibility complex in YACs, Genomics 23 (1994) 520–527.
[6] K. Omori, L. Vergnes, M.M. Zakin, A. Ochoa, The apolipoprotein AICIII–AIV gene cluster: sequence of the ApoCIII–ApoAIV intergenic region, Gene 159 (1995) 231–234.
[7] P. Qiu, L. Benbow, S. Liu, J.R. Greene, L. Wang, Analysis of a human brain transcriptome map, BMC Genom. 3 (2002) 10.
[8] J.D. Barrans, et al., Chromosomal distribution of the human cardiovascular transcriptome, Genomics 81 (2003) 519–524.
[9] K. Kunzelmann, M. Mall, Electrolyte transport in the mammalian colon: mechanisms and implications for disease, Physiol. Rev. 82 (2002) 245–289.
[10] P. de Santa Barbara, G.R. van den Brink, D.J. Roberts, Development and differentiation of the intestinal epithelium, Cell. Mol. Life Sci. 60 (2003) 1322–1332.
[11] E.E. Eichler, D. Sankoff, Structural dynamics of eukaryotic chromosome evolution, Science 301 (2003) 793–797.
[12] R.A. Gibbs, et al., Genome sequence of the Brown Norway rat yields insights into mammalian evolution, Nature 428 (2004) 493–521.
[13] T. Yamashita, et al., Comprehensive gene expression profile of a normal human liver, Biochem. Biophys. Res. Commun. 269 (2000) 110–116.

GASTROENTEROLOGY 2005;128:449–462

La Protein Is a Potent Regulator of Replication of Hepatitis C Virus in Patients With Chronic Hepatitis C Through Internal Ribosomal Entry Site–Directed Translation

MASAO HONDA, TAKEO SHIMAZAKI, and SHUICHI KANEKO
Department of Gastroenterology, Kanazawa University Graduate School of Medicine, Kanazawa, Japan

Background & Aims: Translation of hepatitis C virus is an essential step of viral replication and is mediated by an internal ribosome entry site. We previously reported that the hepatitis C virus internal ribosome entry site is most active during the synthetic (S) or mitotic (M) phases and lowest during quiescent (G_0) phase. Here, we investigated host factors responsible for the regulation of the hepatitis C virus internal ribosome entry site. *Methods:* We synchronized the cell-cycle progression and evaluated gene-expression dynamics of host factors and kinetics of hepatitis C virus internal ribosome entry site activity in cells at various points during the cell cycle by using a complementary DNA microarray. We also validated the significance of identified host factors on hepatitis C virus replication in vivo. *Results:* Hepatitis C virus internal ribosome entry site activity correlated with a gene cluster induced in the S and G_2/M phases. It is interesting to note that most initiation factors known to bind or interact with the hepatitis C virus internal ribosome entry site [poly(rC)-binding protein 2, polypyrimidine tract binding protein, eukaryotic initiation factor 3, eukaryotic initiation factor 2γ, eukaryotic initiation factor 2β, La protein, and heterogenous nuclear ribonucleoprotein L] were induced during the S and G_2/M phases. Expression of La protein, polypyrimidine tract binding protein, and eukaryotic initiation factor 3 (p116, p170) were predominantly repressed in G_0 phase and induced in S and G_2/M phases. Suppression or overexpression of La protein and polypyrimidine tract binding protein in RCF-26 significantly changed hepatitis C virus internal ribosome entry site activity. In the livers of patients with chronic hepatitis C, expression of La protein was significantly increased and correlated with the amount of hepatitis C virus RNA. *Conclusions:* Hepatitis C virus uses host factors induced during cell division but not during quiescence for replication. Of these, La protein is a potent regulator and enhances hepatitis C virus replication in regenerating hepatocytes in patients with chronic hepatitis C.

Hepatitis C virus (HCV), a positive-strand enveloped RNA virus, belongs to the genus *Hepacivirus* of the family Flaviviridae.[1] The human liver infected with HCV develops chronic hepatitis, cirrhosis, and, in some instances, hepatocellular carcinoma.[1,2] Although a combination of ribavirin and interferon has become a popular means of treating infected patients, the results are often unsatisfactory, especially in patients with a high viral load.[3–6] Identification of host factors that regulate HCV replication in infected patients could be helpful in the development of a novel antiviral treatment strategy.

Translation of the polyproteins of the HCV RNA genome is an essential step in viral replication and is supposed to be a fruitful target of new antiviral treatment strategies, such as antisense oligonucleotide (oligo) or small interference RNA. Translation of HCV is initiated by a highly structured RNA segment, the internal ribosome entry site (IRES), that occupies most of the 5′-nontranslated (5′-NTR) RNA.[7–15] The translation machinery of HCV is simple and, because it is a prokaryote, requires only the ribosomal 40S subunit, the eukaryotic initiation factor (eIF)2/guanosine triphosphate/Met-transfer RNA complex, and eIF3 to initiate translation.[7] In contrast, cap-dependent translation is more complex and requires additional canonical initiation factors, such as eIF4E, eIF4G, eIF4A, and eIF4B.[7] Many other noncanonical translation initiation factors, such as La protein,[16,17] polypyrimidine tract binding protein (PTB),[18] heterogeneous nuclear ribonucleoprotein L (RNPL),[19] poly(rC)-binding protein (PCBP)-2,[20] and ribosomal protein S9,[7] interact with HCV IRES and might regulate HCV translation. Thus, the machineries of cap-dependent and HCV IRES–directed translation

Abbreviations used in this paper: CMV, cytomegalovirus; eIF, eukaryotic initiation factor; FBS, fetal bovine serum; FL, firefly luciferase; IRES, internal ribosome entry site; nt, nucleotide; 5′-NTR, 5′ nontranslated region; oligo, oligonucleotide; PABPC, poly(A)-binding protein, cytoplasmic; PCBP, poly(rC)-binding protein; PTB, polypyrimidine tract binding protein; RL, *Renilla* luciferase; RNPL, heterogeneous nuclear ribonucleoprotein L; RTD, real-time detection; RT-PCR, reverse-transcription polymerase chain reaction; SOM, self-organizing map.

© 2005 by the American Gastroenterological Association
0016-5085/05/$30.00
doi:10.1053/j.gastro.2004.11.064

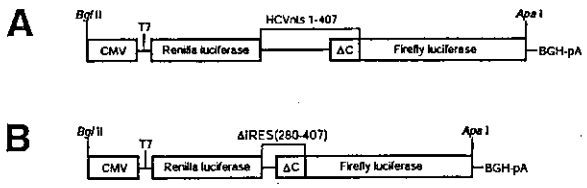

Figure 1. Organization of the transcriptional unit of plasmid pRL-HL and pRL-(ΔIRES)-HL. (*A*) Plasmid pRL-HL[22] contains a dicistronic CMV transcriptional cassette in which upstream *Renilla* and downstream firefly luciferase genes are separated by the complete 5′-NTR and 66-nt core sequence of HCV (nts 1–407; strain 1b) placed in the intercistronic space. (*B*) Plasmid pRL-(ΔIRES)-HL was the control plasmid of pRL-HL in which the functional HCV IRES element (nts 1–279) was deleted. CMV, cytomegalovirus promoter; T7, Bacteriophage T7 RNA polymerase promoter; BGH-pA, bovine growth hormone polyadenylation signal.

can be differentiated in terms of requirements for canonical and noncanonical initiation factors.[21]

We previously found that HCV IRES activity varies during the cell cycle and is greatest during the synthetic (S) or mitotic (M) phases and lowest during the quiescent (G_0) phase.[22] These findings suggest that HCV translation is regulated by cellular proteins that vary in abundance during the cell cycle and that viral replication is enhanced by factors that stimulate the regeneration of hepatocytes in patients with chronic hepatitis C. This finding implies that inflammation and the resulting increased turnover in hepatocytes may increase the number of actively dividing hepatocytes, resulting in increased IRES activity and enhanced HCV replication.

This study profiles the expression of cellular proteins during cell-cycle progression and identifies factors responsible for cell cycle–dependent HCV IRES–directed translation. We evaluated whether those factors are in fact related to HCV replication in the livers of patients with chronic hepatitis C.

Materials and Methods

Plasmids

Plasmid pRL-HL contains a dicistronic cytomegalovirus (CMV) transcriptional cassette in which an upstream *Renilla* luciferase (RL) gene and a downstream firefly luciferase (FL) gene are separated by the complete 5′-NTR and 66-nucleotide (nt) core sequence of HCV (nts 1–407 of a genotype 1b strain) placed within the intercistronic space[22] (Figure 1*A*). Plasmid pRL-(ΔIRES)-HL was the control plasmid of pRL-HL in which the functional HCV IRES element (nts 1–279) had been deleted (Figure 1*B*). This plasmid was constructed by subcloning the 1.82-kilobase *StuI*/*ApaI* fragment of pRL-HL (containing the deleted HCV IRES element [nts 280–341 of the HCV-1b 5′-NTR sequence and 66 nts of the core sequence] fused directly to FL) into the multiple cloning site of pBluescript IISK (Stratagene, La Jolla, CA). A 1.82-kilobase *NotI*/*ApaI* fragment was subsequently excised from this plasmid and cloned into the *NotI*/*ApaI* site of pRL-HL.

The La expression vector pCMV-La was constructed as previously described.[23] The PTB expression vector pRC/CMV-PTB, the RNPL expression vector pcDNA3-myc-hnRNPL, and the PCBP-1 and PCBP-2 expression vectors pcDNA3-myc-haCP1 and pcDNA3-myc-haCP2 were provided by Dr. Stanley M. Lemon,[24] Dr. Gideon Dreyfuss,[25] and Dr. Stephen A. Liebhaber,[26] respectively. Dr. John W. B. Hershey provided the eIF2γ full-length clone in pSP72.[27] We constructed the eIF2γ expression vector pCMV-eIF2-γ by excising the *Eco*RI and *Eco*RI fragment of full-length coding sequences and cloning into *Eco*RI of pCR 3.1 (Invitrogen, San Diego, CA) under the control of the CMV promoter. Dr. Keith Johnson provided the eIF3 p170 full-length clone in PUC19.[28] We constructed the eIF3 p170 expression vector pCMV-eIF3 p170 by excising the *Kpn*I and *Sna*BI fragment of full-length coding sequences and cloning into *Kpn*I and *Eco*RV of pCR 3.1 under the control of the CMV promoter. The complementary DNA (cDNA) of ribosomal protein S9 was cloned by reverse-transcription polymerase chain reaction (RT-PCR) of total RNA isolated from Huh-7 cells by using sense (5′-ACGGTGGAAGCGGACG-CAACATGCCAGTGG-3′) and antisense (5′-GGGACAG-GTGGACTTAATCCTCCTCCTCGTCG-3′) primers. The resultant cDNA was cloned into the TOPO TA cloning vector (Invitrogen), and nt sequences were confirmed. The expression vector pCMV-S9 was constructed by excising and cloning *Hind*III and *Xho*I fragments from TOPO TA into the same sites of pCR 3.1.

Cell Lines

The RCF-26 was a stably transformed cell line from Huh-7 cells (human hepatocellular carcinoma cells) that constitutively express dicistronic RNA transcripts containing sequences encoding 2 reporter proteins, RL and FL, separated by a functional HCV IRES[22] (Figure 1*A*). The ΔRCF-9 was a stably transformed cell line from Huh-7 cells that constitutively expressed dicistronic RNA transcripts in which the functional HCV IRES element (nts 1–279) had been deleted (Figure 1*B*).

Overexpression of Canonical and Noncanonical Initiation Factors in RCF-26

The RCF-26 cells were cultured in Dulbecco's modified Eagle medium (Gibco BRL, Gaithersburg, MD) containing 10% fetal bovine serum (FBS), 1% penicillin/streptomycin, and 400 μg/mL of Geneticin (active compound) (Gibco BRL, Gaithersburg, MD). Cells cultured in a 5% CO_2 incubator at 37°C were transfected with 0.5–1.0 μg of plasmid DNA by using FuGENE 6 (Roche Molecular Biochemicals, Basel, Switzerland) according to the manufacturer's instructions. After 24–48 hours of transfection, the cells were harvested, and reporter genes were assayed.

Reporter Gene Assays

Cells cultured in 10- or 15-cm dishes in Dulbecco's modified Eagle medium containing 10% FBS were trypsinzed. A quarter of the cells were lysed in 1 mL of passive lysis buffer (25 mmol/L Tris-phosphate [pH 7.8], 2 mmol/L dithiothreitol, 2 mmol/L 1,2-diaminocyclohexane-N,N,N′,N′-tetraacetic acid, 10% glycerol, and 1% Triton X-100). RL and FL activities were measured in 20 μL of cell lysate by using the Dual-Luciferase Reporter Assay System (Promega, Madison, WI). Total RNA was isolated from the remainder and processed for analysis by cDNA microarray, Northern blotting, and real-time detection (RTD) PCR.

Antisense Oligodeoxynucleotide

We designed respective antisense phosphorothioate oligos that were complementary to the sequence from 5 nts upstream to 15 downstream of the predicted translational initiation site of the La protein, PTB, eIF3 p170, eIF2γ, RNPL, poly(A)-binding protein, cytoplasmic 1 (PABPC-1), PCBP-2, and ribosomal protein S9 gene. The nt sequences of antisense oligos were 5′-GCCATTACGGCTATCTTTAA-3′ for La protein, 5′-TCCATGGCACACAGAGCAGA-3′ for PTB, 5′-GGCATTTTCCGGCCTCTGAA-3′ for eIF3 p170, 5′-CCAGCTTCTCCGCCCGCCAT-3′ for eIF2γ, 5′-ACCATCGCTCCCGACCGCCT-3′ for RNPL, 5′-TTCATCTCGGCACGGCTGCC-3′ for PABPC-1, 5′-TCCATGTCGAGCAGTGTTCT-3′ for PCBP-2, and 5′-GGCATGTTGCGTCCGCTTCCGCC-3′ for ribosomal protein S9. Positive and negative controls consisted of an antisense oligo for the 5′ region of HCV (nt 330–350), 5′-GTGCTCATGGTGCACGGTCT-3′,[29] and the randomized oligo, 6961, 5′-TACGTTTCTATGTCGATGGG-3′,[29] respectively. Oligodeoxynucleotides (0.5–1.0 μmol/L) were added to the medium by using the FuGENE6 transfection reagent (Boehringer Mannheim, Mannheim, Germany), and the cultures were incubated for 24 hours. Cells were harvested, and HCV IRES activity was evaluated by assaying the reporter genes. To validate repressed targeted gene expression, 1 μg of total RNA was amplified by RT-PCR with specific primers for La protein, PTB, eIF3 p170, and ribosomal protein S9. The internal control was the level of β-actin expression.

Synchronization of Cell Growth and Analysis of Cellular DNA Content

To examine the relationship between HCV IRES–directed translation and cell growth, RCF-26 cells and ΔRCF-9 cells were incubated in 15-cm dishes with low serum or at confluence for 24–48 hours. RCF-26 cells and ΔRCF-9 cells in 10-cm dishes were synchronized at the G_1/S phase border by starvation for 24 hours in medium containing 0.1% FBS, followed by a wash and an 18-hour incubation in medium containing 10% FBS and 2.5 μg/mL aphidicolin. Aphidicolin was removed from the synchronized cells by washing and adding fresh medium containing 1% FBS. The cells were harvested at 3-hour intervals over 48 hours to assess the cell-cycle phase and reporter enzyme activities. The cell-cycle phase distribution in each sample cell population was determined by measuring the DNA content of individual cells by flow cytometry.[22]

Complementary DNA Microarray Analysis

We profiled gene expression in cells at different phases of the cell cycle by cDNA microarray analysis. We reconstructed the gene set of cDNA microarray slides containing 1080 cDNA clones[30] by adding canonical and noncanonical initiation factors. The new microarray included La protein,[16] PTB,[18] eIF2β,[31] eIF2γ,[31] eIF3 p116, eIF3 p170,[32] RNPL,[19] ribosomal protein S9,[7] PCBP-2,[20] PABPC-1,[33] and cell division cycle 2–like 1 (PITSLRE proteins)[34] that bind HCV or other viral IRES structures and might affect the IRES activity. Other canonical initiation factors, such as eIF1A, eIF2A, eIF4A, eIF4B, eIF4E, and eIF5,[7,21,35] were also included to analyze cap-dependent translation machinery.

Total RNA (50 μg) isolated from serum-starved or confluent cells (10% FBS and at 60%–70% cell density) was labeled with a fluorescent dye for the cDNA microarray.[30,36,37] To profile gene expression in cells during the cell cycle, total RNA was periodically extracted from synchronized cells at 3, 9, 15, 18, 24, 30, 36, and 42 hours released from aphidicolin block (G_1/S border). After 1 round of amplification, antisense RNA was labeled and hybridized with the cDNA microarray.[30,36,37] Images were acquired, and cDNA microarray slides were analyzed as previously described.[30,36,37] A 1-dimensional self-organizing map (SOM) was constructed to cluster genes with a similar expression profile throughout cell-cycle progression (Cluster and Tree view; http://www.microarrays.org.html/software).

Northern Blotting

We evaluated La protein, PTB, and albumin expression in cultured cells and in tissue samples by Northern blotting. Total RNA (20 μg) was separated on denaturing agarose/formaldehyde gels, transferred to a membrane, and hybridized with specific probes under standard conditions.

Western Blotting

RCF-26 cells seeded in a 10-cm dish were grown to subconfluency and washed twice with phosphate-buffered saline. Cells were lysed in radioimmunoprecipitation assay buffer. Cell lysates were collected by pelleting cell debris, and the concentration of protein was quantified by using a dye-binding assay (Bio-Rad, Hercules, CA). Eighty micrograms of cell lysate was electrophoresed in a sodium dodecyl sulfate/12.5% polyacrylamide gel and electrotransferred to a nitrocellulose membrane. After blocking with phosphate-buffered saline with 0.3% Tween-20 containing 5% skim milk for 1 hour, the membranes were reacted with appropriate antibodies. After washing with phosphate-buffered saline with 0.3% Tween-20, membranes were reacted with horseradish peroxidase–conjugated anti-mouse immunoglobulin G or anti-rab-

bit immunoglobulin G antibodies diluted 1:3000. Membranes were washed again and then visualized with an enhanced chemiluminescence kit (Amersham Pharmacia Biotech, Uppsala, Sweden).

Real-Time Detection Polymerase Chain Reaction

The PCR reaction mixture was prepared by using TaqMan Universal Master Mix (PE Applied Biosystems, Foster City, CA). The primer set applied to amplify La protein messenger RNA (mRNA) consisted of 5′-CGCTGGGAGGTGGAGTCGTT-3′ (exon 1) and 5′-CCCGTGGCAAATTGAAGTCG-3′ (exon 2). The probe, 5′-TGCCCTGGAGGCCAAAATCTGTCATC-3′ (exon 2), was designed to target an internal region between the forward and reverse primers. The primer set for PTB mRNA was 5′-AGCACGCCAAGCTGTCGCT-3′ (exon 8) and 5′-GGAACGGAAAGGCCGAAGG-3′ (exons 8–10). The probe was 5′-ACACACGCCCAGACCTGCCTTCCG-3′ (exon 8). The primer set for eIF3 p170 protein mRNA was 5′-CCGGAAAATGCCCTCAAACTA-3′ (exon 1) and 5′-AAGTGGCTCTTGCGAAGATCCACGC-3′ (exon 7). The probe sequence was 5′-CCAACGAATTTCTTGAGGTT-3′ (exon 2). The primer set for the internal control glyceraldehyde-3-phosphate dehydrogenase mRNA was designed according to GenBank M33197 by using the following primers: exon 7, 5′-TGCACCACCAACTGCTTAGCACCC-3′; and exon 8, 5′-CTTGATGTCATCATATTTGGCAGG-3′. The probe for glyceraldehyde-3-phosphate dehydrogenase-P, designed on the basis of exons 7 and 8, was 5′-TGACCACAGTCCATGCCATCACTGC-3′. Fifty PCR amplification cycles of 95°C for 30 seconds, 60°C for 40 seconds, and 72°C for 30 seconds were repeated by using a real-time PCR system (ABI PRISM 7700 Sequence Detection System; PE Applied Biosystems). To prepare standard RNA, PCR products were cloned into pBluescript vector and linearized at the T3 promoter site. Standard RNA was synthesized by using T7 RNA polymerase and purified by using Isogen (Wako Junyaku, Osaka, Japan) and deoxyribonuclease I (TaKaRa, Shiga, Japan). We detected HCV RNA in liver by using RTD-PCR as previously described.[38]

Statistical Analysis

All data are expressed as means ± SEM. Significance was tested by the Student *t* test and 1-way analysis of variance with Bonferroni's methods.

Results

Gene-Expression Profiling in Confluent or Serum-Starved Cells and the Activities of Hepatitis C Virus Internal Ribosomal Entry Site–Directed Translation

RCF-26 cell lines constitutively express dicistronic RNA transcripts containing sequences encoding the reporter proteins RL and FL separated by a functional HCV IRES (Figure 1). The activities of these proteins expressed in RCF-26 cells reflect cap-dependent and HCV IRES–directed translation, respectively. To rule out the possibility that FL activity from the second cistron reflected the nonspecific ribosomal scanning rather than HCV IRES–directed translation, we evaluated RL and FL activities in ΔRCF-9 cells in which the functional HCV IRES element had been deleted. The ratio of FL to RL (relative HCV IRES activity) in ΔRCF-9 was 2.5% of that in RCF-26, thus reflecting the specificity of HCV IRES activity in RCF-26 cells (Figure 2*B–D*).

To examine the relationship of the cellular proteins that vary in abundance and HCV IRES activities, RCF-26 cells and ΔRCF-9 cells were cultured in 15-cm dishes at confluence or under serum depletion for 48 hours, and changes in cellular gene expression and HCV IRES activities were evaluated. Under these conditions, the cellular DNA content increased at G_0/G_1 phase (49% to 74% in confluent cells and to 59% in serum-starved cells) and decreased at S phase (38% to 18% in confluent cells and to 35% in serum-starved cells) or G_2/M phase (14% to 8% in confluent cells and to 6% in serum-starved cells; Figure 2*A*). The degree of changes during the cell cycle was much greater in the confluent cells than in the serum-starved cells. The activities of HCV IRES–directed translation were reduced to 24% in confluent cells and to 22% in serum-starved cells compared with controls (Figure 2*C* and *D*), whereas the activities of cap-dependent cellular translation were essentially maintained (Figure 2*B*). Neither a significant difference in FL activity nor relative HCV IRES activity was found in ΔRCF-9 under these conditions (Figure 2*C* and *D*).

These results were not due to variations in the RNA stability of the RL and FL reporter genes. Northern blotting of mRNA transcribed from dicistronic constructs containing sequences encoding these 2 reporter proteins did not show either RNA degradation or splicing (data not shown). The relative expression ratio of mRNA of RL to FL determined by cDNA microarray did not change in either confluent or serum-starved cells (Figure 2*E*).

Gene-expression profiling changed in response to these conditions listed in Table 1. Serum proteins such as α_2-macroglobulin and albumin, as well as cell adhesion molecules such as cadherin, major histocompatibility complex, and fibronectin, were up-regulated by more than 1.8-fold. Albumin, a major serum protein that is specifically produced in the liver, was remarkably regulated in a cell-cycle dependent manner. However, cell-cycle and growth-related genes such as cyclin A, cyclin B, CDK1, cell division cell cycle 18, p53, hepatoma-

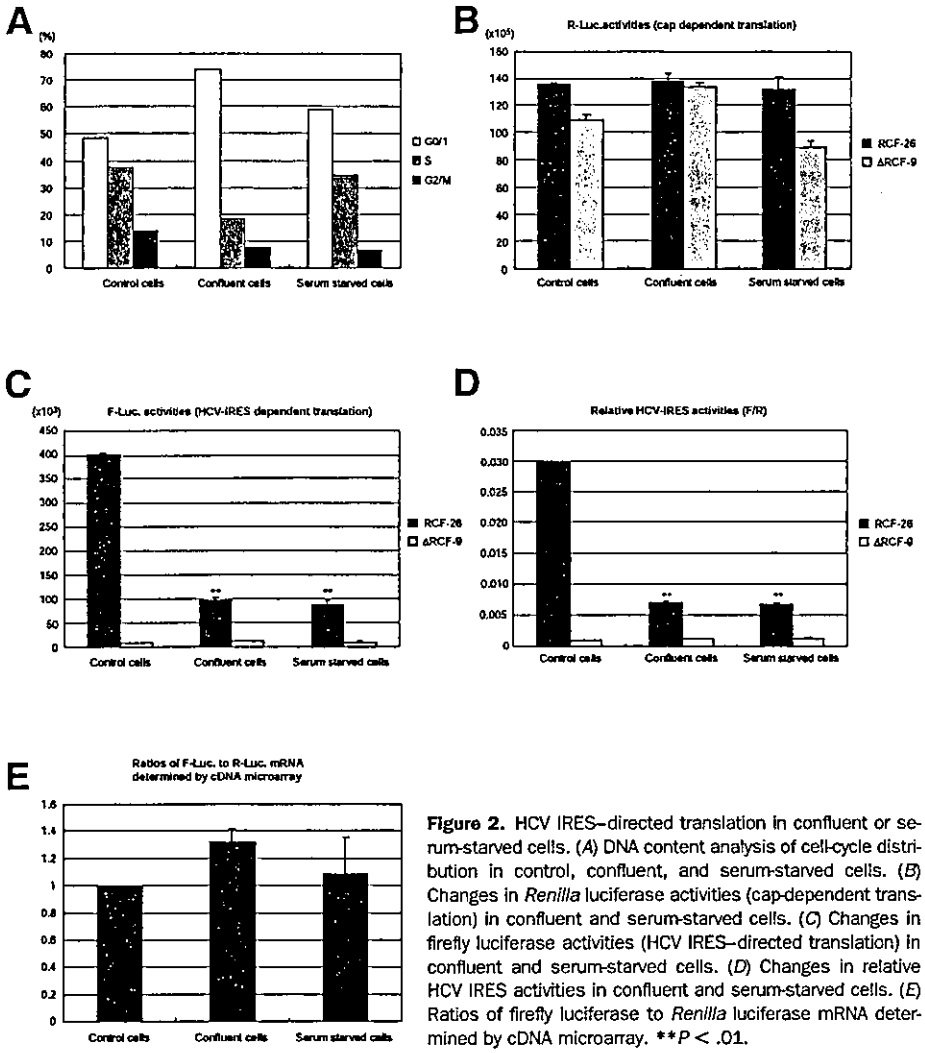

Figure 2. HCV IRES–directed translation in confluent or serum-starved cells. (*A*) DNA content analysis of cell-cycle distribution in control, confluent, and serum-starved cells. (*B*) Changes in *Renilla* luciferase activities (cap-dependent translation) in confluent and serum-starved cells. (*C*) Changes in firefly luciferase activities (HCV IRES–directed translation) in confluent and serum-starved cells. (*D*) Changes in relative HCV IRES activities in confluent and serum-starved cells. (*E*) Ratios of firefly luciferase to *Renilla* luciferase mRNA determined by cDNA microarray. $^{**}P < .01$.

derived growth factor, and nm23 were down-regulated, as were genes related to RNA polymerase, such as RNA polymerase II, subunit 5-mediating protein (RMP), La protein, and topoisomerase II. The La protein binds the stem loop IV structure in HCV IRES and stimulates HCV IRES–directed translation.[16,17] With regard to changes in the expression of canonical and noncanonical initiation factors (Table 2), La protein and PTB expression were repressed in both confluent and serum-starved cells. The expression of eIF3 (p170 and p116) was predominantly repressed in confluent cells, and the expression of eIF2γ was predominantly repressed in serum-starved cells. Conversely, the expression of ribosomal protein S9 and PABPC-1 was induced in confluent cells. The degree to which gene expression changed was more predominant in confluent cells than in serum-starved cells. This might reflect the greater degree of changes in the cell-cycle distribution of G_0/G_1 and S phases in confluent cells than in serum-starved cells (Figure 2*A*). The results of northern blots of La protein, PTB, and albumin expression coincided with these results (Figure 3). We evaluated changes in La protein and PTB expression by using RTD-PCR. The relative expression of La protein in confluent and serum-starved cells was 16% and 33% of control cells, respectively. The relative expression of PTB in confluent and serum-starved cells was 10% and 26% of control cells, respectively (data not shown). These data suggest that several canonical and noncanonical initiation factors, such as La protein, PTB, eIF3, and eIF2γ, are initiation factors responsible for regulating HCV IRES activity in a cell cycle–dependent manner.

Table 1. Up- and Down-regulated Genes in Confluent and Serum-Starved Cells

UniGene	Gene name	Category	Confluent cells	Serum-starved cells	Mean (fold)
Up-regulated					>1.8
Hs.74561	Alpha-2-macroglobulin	Serum protein	12.87 ± 2.13	5.13 ± 0.10	9.00 ± 2.40
Hs.75442	Albumin	Serum protein	6.07 ± 1.07	3.26 ± 0.37	4.67 ± 0.93
Hs.77054	B-cell translocation gene 1	Antiproliferative gene	4.73 ± 1.76	2.97 ± 0.83	3.85 ± 0.94
Hs.82004	Cadherin 1, E-cadherin (epithelial)	Cell adhesion	5.14 ± 2.46	2.36 ± 0.30	3.75 ± 1.29
Hs.2257	Vitronectin	Cell adhesion	3.97 ± 0.68	2.11 ± 0.22	3.04 ± 0.61
Hs.277477	MHC class IC	Cell adhesion	3.26 ± 0.82	2.17 ± 0.09	2.71 ± 0.46
Hs.77961	MHC class IB	Cell adhesion	3.33 ± 0.23	2.08 ± 0.24	2.71 ± 0.39
Hs.1119	TR3 orphan receptor	Receptor	3.38 ± 1.23	1.95 ± 0.23	2.66 ± 0.66
Hs.1665	Zinc finger transcriptional regulator	Transcription factor	2.66 ± 0.40	2.53 ± 0.40	2.60 ± 0.23
Hs.287820	Fibronectin gene	Cell adhesion	2.40 ± 0.77	2.11 ± 0.34	2.26 ± 0.36
Hs.2780	JunD	Oncogene	2.23 ± 0.39	1.99 ± 0.54	2.11 ± 0.28
Down-regulated					<0.55
Hs.89525	Hepatoma-derived growth factor	Cell growth	0.67 ± 0.27	0.42 ± 0.08	0.55 ± 0.13
Hs.7943	RMP	RNA polymerase II binding	0.44 ± 0.09	0.64 ± 0.07	0.54 ± 0.07
Hs.23960	Cyclin B	Cell cycle	0.44 ± 0.25	0.62 ± 0.17	0.53 ± 0.13
Hs.118638	Nm23A	Cell growth	0.52 ± 0.01	0.53 ± 0.11	0.52 ± 0.05
Hs.83715	Autoantigen La	RNA polymerase III synthesis	0.43 ± 0.06	0.61 ± 0.01	0.52 ± 0.06
Hs.16297	COX17	Cytochrome-c-oxidase	0.47 ± 0.14	0.55 ± 0.06	0.51 ± 0.07
Hs.95577	CDK1	Cell cycle	0.36 ± 0.02	0.65 ± 0.07	0.50 ± 0.09
Hs.174017	Topoisomerase (DNA) II alpha	RNA polymerase II holoenzyme	0.44 ± 0.11	0.55 ± 0.08	0.50 ± 0.05
Hs.85137	Cyclin A	Cell cycle	0.42 ± 0.03	0.56 ± 0.17	0.49 ± 0.08
Hs.9235	Nucleoside-diphosphate kinase	Cell growth	0.51 ± 0.08	0.46 ± 0.05	0.49 ± 0.04
Hs.75133	Transcription factor 6–like 1	Transcription factor	0.40 ± 0.07	0.57 ± 0.18	0.48 ± 0.09
Hs.69563	Cell division cycle 18	Cell cycle	0.45 ± 0.04	0.51 ± 0.09	0.48 ± 0.04
Hs.58593	RAP30	Transcription factor	0.37 ± 0.02	0.58 ± 0.00	0.48 ± 0.06
Hs.75323	Prohibitin	Antiproliferative gene	0.50 ± 0.01	0.39 ± 0.01	0.44 ± 0.03
Hs.1846	p53	Cell cycle	0.66 ± 0.18	0.22 ± 0.04	0.44 ± 0.15
Hs.111758	Keratin 6	Housekeeping	0.24 ± 0.02	0.63 ± 0.07	0.43 ± 0.12
Hs.78271	Keratin 8	Housekeeping	0.33 ± 0.18	0.53 ± 0.08	0.43 ± 0.10
Hs.748	Fibroblast growth factor receptor 1	Cell growth	0.39 ± 0.12	0.30 ± 0.05	0.34 ± 0.06

Hepatitis C Virus Internal Ribosome Entry Site Activity at Different Phases of the Cell Cycle

We examined the relationship between HCV IRES activity and cell division in more detail. We synchronized cell-cycle progression and compared the production of RL and FL reporter proteins during different phases of the cell cycle. Cells were blocked at the G_1/S interface by adding aphidicolin to the culture medium and were then released from the aphidicolin

Table 2. Up- and Down-regulated Initiation Factors in Confluent and Serum-Starved Cells

UniGene	Gene name	Confluent cells	Serum-starved cells	Mean (fold)
Hs.180920	Ribosomal protein S9	1.92 ± 0.01	1.11 ± 0.18	1.51 ± 0.24
Hs.172550	Polypyrimidine tract binding protein (PTB)	0.62 ± 0.17	0.62 ± 0.03	0.62 ± 0.07
Hs.83715	La protein	0.43 ± 0.06	0.61 ± 0.01	0.52 ± 0.06
Hs.2730	Heterogeneous nuclear ribonucleoprotein L (RNPL)	1.23 ± 0.33	1.02 ± 0.13	1.13 ± 0.16
Hs.63525	Poly(rC)-binding protein 2 (PCBP2)	1.20 ± 0.11	0.95 ± 0.10	1.07 ± 0.09
Hs.172182	Poly(A)-binding protein, cytoplasmic 1	1.87 ± 0.62	1.19 ± 0.05	1.53 ± 0.32
Hs.183418	Cell division cycle 2–like 1 (PITSLRE proteins)	0.85 ± 0.10	0.70 ± 0.07	0.78 ± 0.07
Hs.198899	eIF3-p170	0.47 ± 0.28	1.10 ± 0.36	0.79 ± 0.26
Hs.57783	eIF3-p116	0.58 ± 0.12	0.70 ± 0.02	0.64 ± 0.06
Hs.4310	eIF1A	0.84 ± 0.06	0.89 ± 0.17	0.86 ± 0.07
Hs.151777	eIF2A	1.37 ± 0.20	1.59 ± 0.20	1.48 ± 0.13
Hs.12163	eIF2β	0.88 ± 0.10	0.94 ± 0.02	0.91 ± 0.04
Hs.211539	eIF2γ	1.31 ± 0.03	0.61 ± 0.17	0.96 ± 0.22
Hs.129673	eIF4A	1.05 ± 0.09	0.81 ± 0.07	0.93 ± 0.08
Hs.93379	eIF4B	1.38 ± 0.48	0.94 ± 0.20	1.16 ± 0.25
Hs.79306	eIF4E	0.86 ± 0.14	0.83 ± 0.01	0.84 ± 0.06
Hs.286236	eIF5	0.91 ± 0.02	1.23 ± 0.35	1.07 ± 0.17

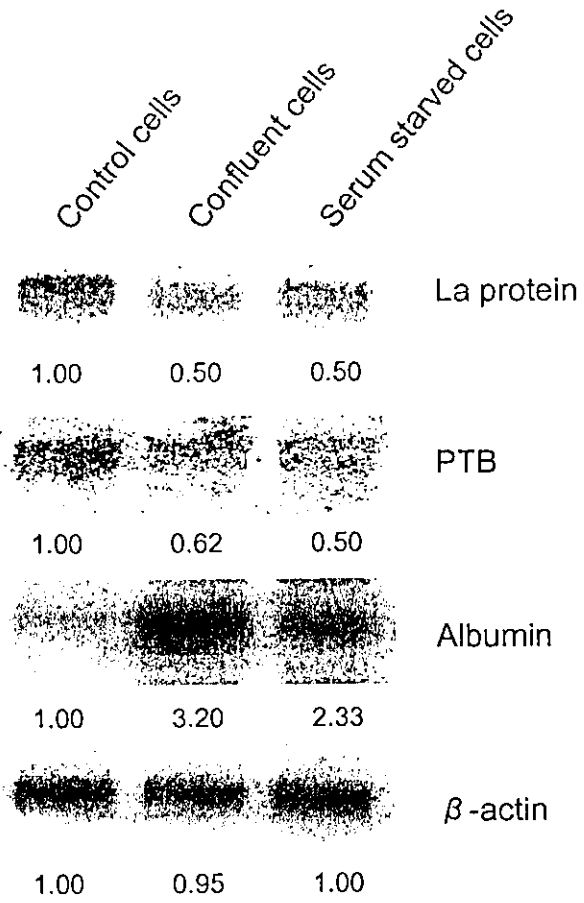

Figure 3. Northern blotting of La protein, PTB, and albumin in RCF-26. Expression of La protein and PTB is repressed in confluent and serum-starved cells, whereas albumin expression is significantly up-regulated.

block. Synchronized cells subsequently moved into the S and G_2/M phases of the cell cycle and then returned to G_1/S phase at approximately 27 hours, as determined by the cellular DNA content measured by flow cytometry (Figure 4*A*). RL activities increased proportionally, reflecting the increased number of cells after division. The cell number doubled at approximately 27 hours after 1 round of the cycle was completed. Conversely, HCV IRES activity varied with cell cycle, and the ratio of FL to RL (relative HCV IRES activity) increased during and immediately after G_2/M phase (12–18 hours after release from aphidicolin). The relative HCV IRES activity decreased by 36 hours after release (Figure 4*C*), corresponding to reentry into the G_0 and G_1 phases. However, the HCV IRES activity increased again, starting at approximately 39 hours, probably because many cells continued into a second cycle (Figure 4*A* and *C*). No significant differences in relative HCV IRES activity were found in ΔRCF-9 cells up to 30 hours after release (Figure 4*C*).

Gene-Expression Profiles in Cells Undergoing Cell-Cycle Progression

To determine which host factors are involved in this cell cycle–dependent regulation of HCV IRES activity, we evaluated gene-expression profiles in cells undergoing cell-cycle progression. Total RNA was extracted from synchronized cells at 3, 9, 15, 18, 24, 30,

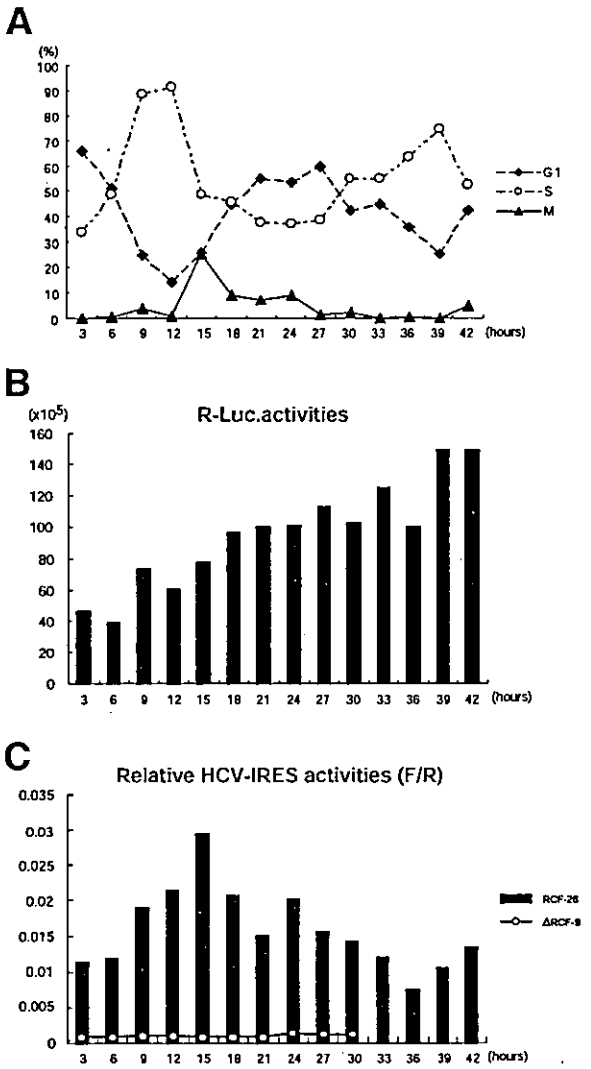

Figure 4. HCV IRES activity and cell-cycle progression. (*A*) Changes in distribution with cell-cycle progression. Proportions of G_1, S, and G_2/M are individually shown. (*B*) Changes of *Renilla* luciferase activities (cap-dependent translation) with cell-cycle progression. (*C*) Changes in relative HCV IRES activities (firefly to *Renilla* luciferase activities; FL/RL) with cell-cycle progression. HCV IRES activity varied with cell cycle in RCF-26 cells but did not change in ΔRCF-9 cells.

36, and 42 hours after release from the aphidicolin block (G_1/S border) and was analyzed with the cDNA microarray. We constructed a 1-dimensional SOM to evaluate changes in gene expression (Cluster and Tree view; http://www.microarrays.org/software/html) (Figure 5). We identified 3 large gene clusters as the cell cycle progressed. The first cluster of genes was induced at S phase (at 3 to 9 hours). The second and third clusters were induced at G_2/M (at 15–18 hours) and at G_1 (at 24 to 36 hours), respectively. Most of the HCV IRES–related canonical and noncanonical initiation factors were induced during S and G_2/M phases. PCBP-2, PTB, eIF3 (p110 and p170), eIF2γ, and eIF2β were induced during S phase, whereas La protein and RNPL were induced during G_2/M. These factors bind HCV IRES structure or have functional relevance to HCV IRES activity. Conversely, PABPC-1, eIF4A, and eIF4B were induced during G_1 phase. These factors are not required for HCV IRES–directed translation but are necessary for cap-dependent translation.[39] The induction of the ribosomal protein S9 in G_1 phase was a controversial finding because S9 was reported to bind stem loop IIId of HCV IRES. The functional role of the ribosomal protein S9 is discussed later. In cells, translation takes place immediately in the presence of mRNA, and luciferase activity could be detected within 30 seconds from the initiation of the translation. Thus, the induction of canonical and noncanonical initiation factors related to HCV IRES during S and G_2/M phases contributed to cell cycle–dependent regulation of translation directed by HCV IRES (Figure 5).

We evaluated changes in La protein expression determined by the cDNA microarray by using RTD-PCR (Figure 6). The changes in HCV IRES–directed translation and in La protein expression closely correlated (Figure 6).

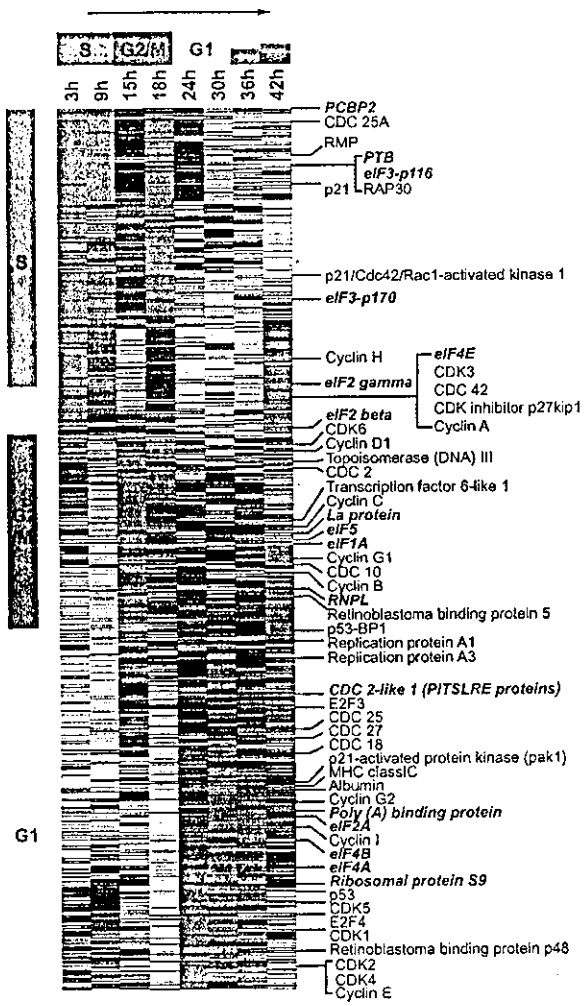

Figure 5. Gene-expression profiling in RCF-26 cells undergoing cell-cycle progression. RCF-26 cells were synchronized at the G_1/S border with aphidicolin. After release from aphidicolin block, the cell cycle progressed to S phase at 3–6 hours and G_2/M phase at 15–18 hours and returned to G_1 phase at 24–30 hours. Cells were harvested at 3, 9, 15, 18, 24, 30, 36, and 42 hours and analyzed with cDNA microarray, and then an SOM was constructed by using Cluster (Stanford University). Gene clusters up-regulated in the S, G_2/M, and G_1 phases (*red*) were detected with cell-cycle progression. Canonical and noncanonical initiation factors and cell cycle–related genes are listed (*right*).

Functional Analysis of the Effect of HCV IRES-Related Canonical and Noncanonical Initiation Factors on Translation Directed by HCV IRES

To prove that the induction of the canonical and noncanonical initiation factors during S and G_2/M phases contributes to cell cycle–dependent translation of HCV, antisense phosphorothioate oligos were designed for La protein, PTB, eIF3 p170, eIF2γ, RNPL, PABPC-1, PCBP-2, and ribosomal protein S9, and HCV IRES activity was evaluated under the suppression of these factors. RT-PCR showed that expression of the targeted factors was significantly reduced by the antisense oligos, whereas that of β-actin did not significantly change (Figure 7*B*). Reduced expression of these factors was also evaluated by Western blotting (Figure 7*C*). The suppression of La protein, PTB, and eIF2γ specifically reduced HCV IRES activity to 40%, 50%, and 53% of the control level, respectively. The effect of inhibiting HCV IRES activity was equal to or greater than that exerted by an antisense oligo against 5′-NTR of HCV (nt 330–350). However, suppression of eIF3 p170, RNPL, PABPC-1, PCBP-2, and ribosomal protein S9 did not reduce HCV IRES activity (Figure 7*A*). To rule out the

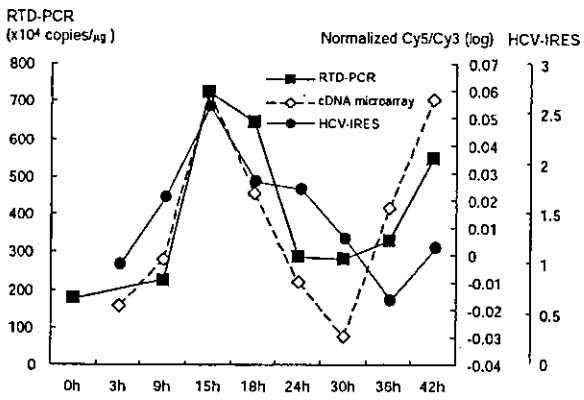

Figure 6. La protein expression in RCF-26 under cell-cycle progression determined by RTD-PCR. Normalized Cy5/Cy3 of mRNA expression of La protein and HCV IRES activities are shown in same dimension.

possibility that these reduced HCV IRES activities were not due to nonspecific suppression by the antisense oligos, antisense oligos to La protein, PTB, eIF3 p170, and ribosomal protein S9 were applied to ΔRCF-9 in which the functional HCV IRES element had been deleted. Two antisense oligos to La protein and PTB, which reduced HCV IRES activity in RCF-26, did not change HCV IRES activity in ΔRCF-9. Similarly, 2 antisense oligos to eIF3 p170 and ribosomal protein S9, which had no effect on HCV IRES activity, did not have any effect on HCV IRES activity in ΔRCF-9 (Figure 7*A*). Conversely, overexpression of La protein, PTB, and eIF3 p170 significantly enhanced HCV IRES activity in a dose-dependent manner, whereas the overexpression of eIF2γ, RNPL, PCBP-1, PCBP-2, and ribosomal protein S9 had no effect (Figure 8). The overexpression of La protein, PTB, and eIF3 p170 in ΔRCF-9 did not have any effect on HCV IRES activity (Figure 8). We also confirmed these findings in rabbit reticulocyte lysates by co-translating pRL-HL (HCV IRES reporter) and La protein, PTB, and eIF3 p170 (data not shown). Thus, of these HCV IRES–related canonical and noncanonical initiation factors, La protein and PTB significantly changed HCV IRES activity in both the suppressed and overexpressed states. Thus, changes in the expression of these factors alter HCV IRES activity in a cell cycle–dependent manner.

Expression of La Protein, Polypyrimidine Tract Binding Protein, and Eukaryotic Initiation Factor 3 in Lesions of Chronic Hepatitis C

To examine the functional role of these factors on HCV replication in the lesions of chronic hepatitis C, we evaluated their expression in 26 liver samples from patients with chronic hepatitis C and in 8 normal liver samples by RTD-PCR. Tables 3 and 4 list the clinical characteristics of the patients. The expression level of La protein in the specimens of the patients with chronic hepatitis C was significantly higher than that of the normal livers, whereas the expression of PTB and eIF3 p170 was not statistically different (Table 3). Some of these samples were also reevaluated by Northern blotting, and the results were similar (data not shown). Up-regulation of the La protein was related to neither the histological stage nor the activity of liver disease (Table 4). However, the expression of La protein was significantly correlated with the amount of HCV RNA in the liver (Figure 9). Moreover, HCV RNA replication was significantly higher in liver with high La protein expres-

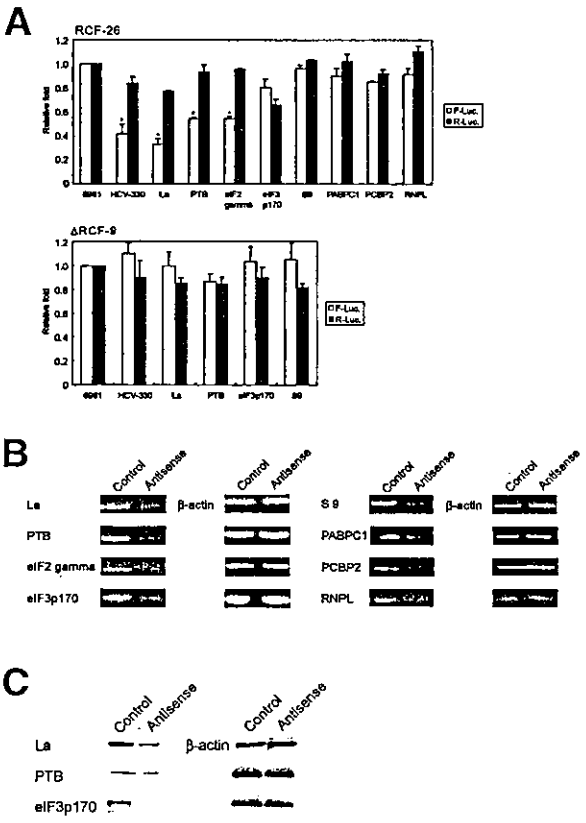

Figure 7. Suppression of HCV IRES–related canonical and noncanonical initiation factors (La protein, PTB, eIF3 [p170], eIF2γ, RNPL, PABPC-1, PCBP-2, and ribosomal protein S9) by specific antisense phosphorothioate oligos and HCV IRES activity in RCF-26 and ΔRCF-9. (*A*) Changes in *Renilla* (cap-dependent translation) and firefly luciferase (HCV IRES–directed translation) activities caused by suppression of these factors by antisense phosphorothioate oligos. $*P < .05$. (*B*) Suppression of factors confirmed by RT-PCR. (*C*) Suppression of factors confirmed by Western blotting.

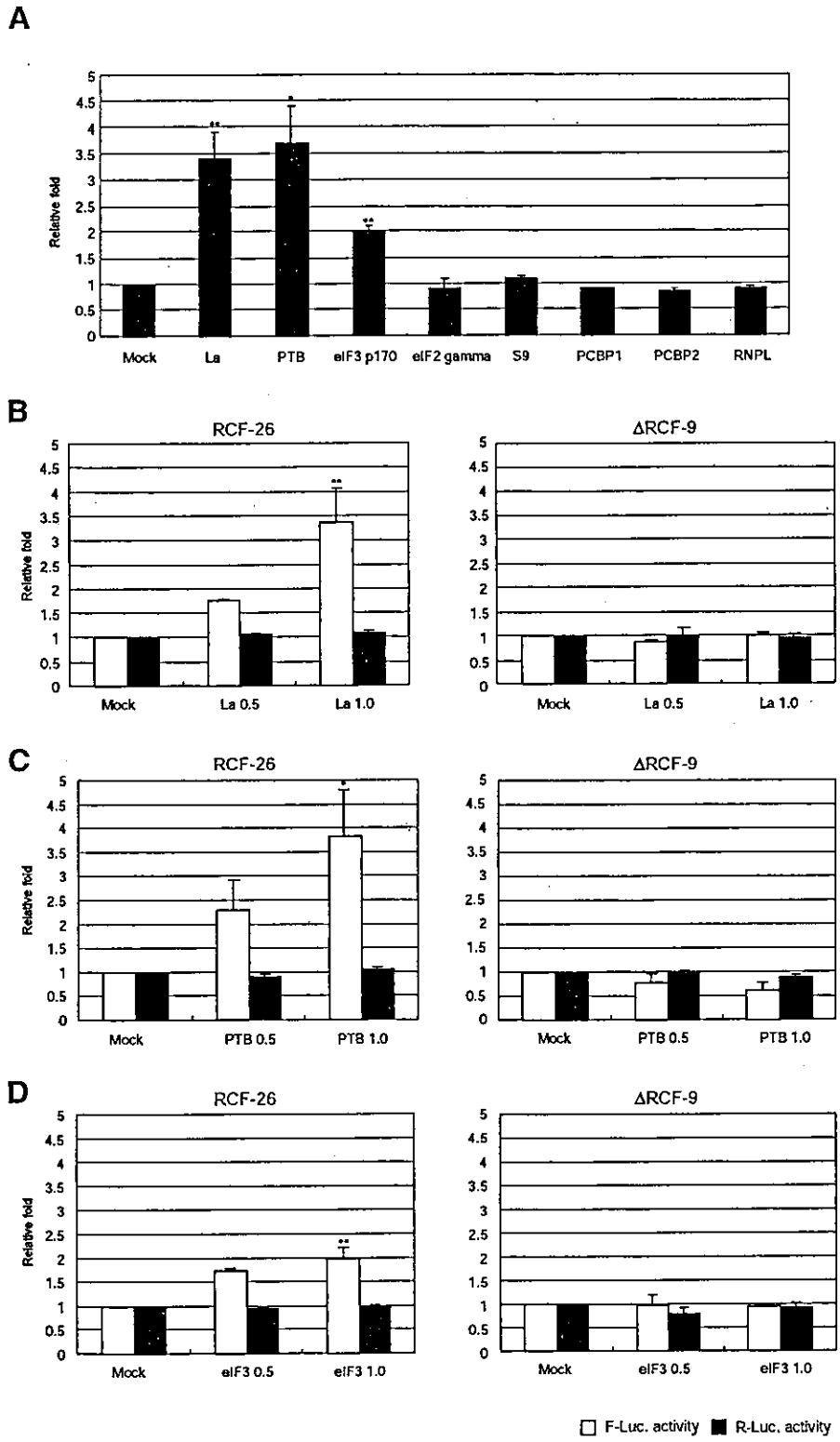

Figure 8. (*A*) Overexpression of HCV IRES–related canonical and noncanonical initiation factors (La protein, PTB, eIF3 [p170], eIF2γ, RNPL, PCBP-1, PCBP-2, and ribosomal protein S9) in RCF-26 and HCV IRES activity. (*B–D*) Dose-dependent overexpression of La protein, PTB, and eIF3 p170 in RCF-26 and ΔRCF-9. $*P < .05$; $**P < .01$.

Table 3. Expression of La Protein, PTB, and eIF3 (p170) in Liver Detected by RTD-PCR

Diagnosis	n	Age (y)	Sex (M:F)	ALT (*IU/L*)	Serological HCV type (group 1:group 2)	La (×10^6 *copies/μg*)	PTB-1 (×10^5 *copies/μg*)	eIF3 (p170) (×10^6 *copies/μg*)
Normal	8	64.5 ± 4.10	5:3	17.0 ± 9.86	ND	1.08 ± 0.11	1.34 ± 0.15	3.32 ± 0.46
Chronic hepatitis C	26	62.8 ± 2.27	20:6	67.7 ± 10.2[a]	21:3[b]	2.75 ± 0.26[c]	1.40 ± 0.14	2.21 ± 0.31

ALT, alanine aminotransferase; ND, not done.
[a]$P < .05$.
[b]Two patients were unclassified.
[c]$P < .01$.

sion (Figure 10). These findings indicate that La protein plays an important role in the replication of HCV in the livers of patients infected with chronic hepatitis C.

Discussion

Although extensive studies have examined the molecular biology of HCV, the responsible host factors that regulate HCV replication in patients with chronic hepatitis C have not yet been elucidated. Patients with a high viral load are refractory to interferon therapy, even when it is combined with ribavirin.[3–6] Recent advances in the HCV replicon system have shown some adaptive mutations in the HCV genome (NS5A or NS3) for efficient replication of cellular factors that inhibit HCV replication, such as PKR and interferon-regulatory protein 1.[40] However, there has been no clear evidence that these factors are truly determinant of HCV replication in patients with chronic hepatitis C. The identification of host factors that regulate HCV replication in vivo should show the underlying mechanism of high viral load in patients with chronic hepatitis C. Moreover, it could provide a basis for the development of a new antiviral treatment strategy.

The translation of viral polyprotein is an important step in viral replication and could thus present a target for a novel antiviral therapy. Translation of the HCV RNA genome is initiated by a highly structured RNA segment, the IRES, that occupies most of the 5′-NTR RNA.[7–15] We showed that HCV IRES activity varies during different phases of the cell cycle: it is highest during the S and M phases and lowest during the G_0 phase of the cell cycle.[22] These findings have important clinical relevance because viral translation might be enhanced by factors that stimulate the regeneration of hepatocytes in patients with chronic hepatitis C. We investigated the molecular basis of these findings and found host factors that regulate HCV IRES.

The expression of La protein, PTB, eIF3, and eIF2γ was repressed in confluent and serum-starved cells, but eIF3 and eIF2γ were reduced in confluent or serum-starved cells. Analysis of cell-cycle progression more precisely showed the interaction of these initiation factors with the cell cycle–dependent regulation of HCV IRES activity. Most of the HCV IRES–related canonical and noncanonical initiation factors (PCBP-2, PTB, eIF3, eIF2γ, eIF2β, La protein, and RNLPL) were induced during the S and G_2/M phases of the cell cycle. Conversely, eIF4A, eIF4B, and PABPC-1, which are not supposed to be a requirement for HCV IRES activity,[33,39] were induced during G_1. In cells, because protein translation takes place immediately in the presence of mRNA, dynamism of expression profiles might directly link to HCV IRES activity, although some protein levels were also regulated by the posttranslational modification. The finding that HCV uses host factors induced during cell division (S and G_2/M), but not during quiescence (G_0/G_1), is of interest. In this respect, HCV IRES–directed translation differed from either cap-dependent or IRES-directed translation by encephalomyocarditis virus and the picornavirus-like group. Reports indicate that eIF4B and PABPC-1 are required for encephalomyocarditis virus and poliovirus, but not for HCV translation.[39] G_1 induction of the ribosomal protein S9, which supposedly binds the secondary structure of HCV IRES,[7] seems controversial. To further investigate these findings, we evaluated the functional roles of these factors in HCV IRES activity. Among the canonical and noncanonical HCV IRES–related initiation factors, the suppression of PTB, La protein, and eIF2γ by using antisense oligos reduced HCV IRES activity, and the overexpression of PTB, La, and eIF3 stimulated HCV IRES activity. The La protein and PTB changed HCV IRES activity in both

Table 4. Histological Findings and La Protein Expression

Histology	n	La (×10^6 *copies/μg*)
F1	2	1.98 ± 0.03
F2	6	3.31 ± 0.80
F3	7	3.04 ± 0.48
F4	11	2.40 ± 0.30
A1	10	2.72 ± 0.52
A2	15	2.82 ± 0.30
A3	1	1.86

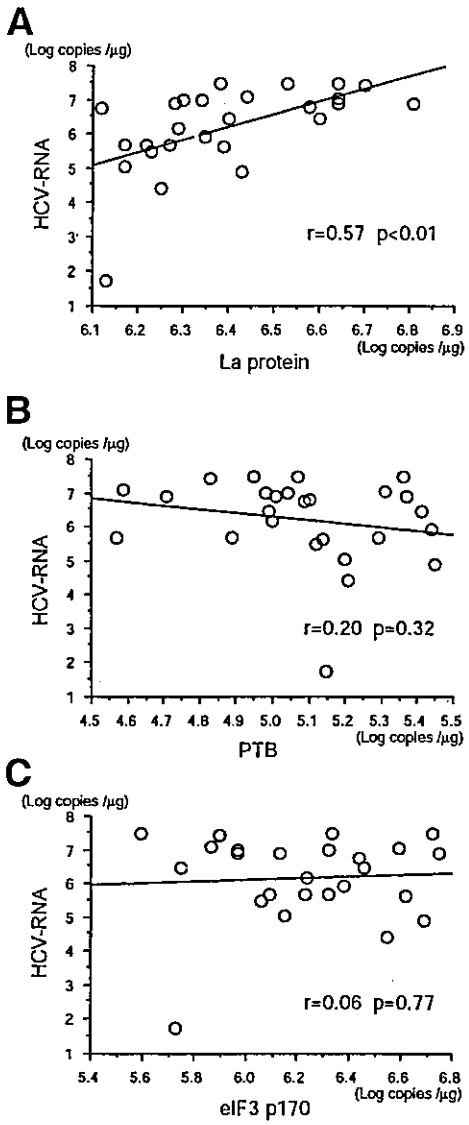

Figure 9. Correlation of La protein (*A*), PTB (*B*), and eIF3 p170 (*C*) with the amount of HCV RNA in tissue lesions of chronic hepatitis C.

the suppressed and overexpressed states. However, neither suppression nor overexpression of ribosomal protein S9 affected HCV IRES activity. Thus, this study could not identify the functional significance of ribosomal protein S9 for HCV IRES activity.

The definition of these initiation factors has very important clinical relevance to HCV replication. We therefore investigated the expression of La protein, PTB, and eIF3 in tissue lesions from patients with chronic hepatitis C. Expression of La protein was significantly increased in the liver of patients, whereas that of PTB and eIF3 did not significantly increase. Neither histological activity nor stage was associated, but the amount of liver HCV RNA was significantly correlated with the level of La protein expression. Patients that expressed high levels of La protein in the liver were infected with more HCV (Figure 10). Thus, La protein plays an important role in HCV replication in livers of patients with chronic hepatitis C. Two possible mechanisms might explain the induction of La protein in the livers of chronic hepatitis C patients. First, significant proportions of cells undergo division during hepatocyte regeneration, and the proportion of cells in M phase that lead to the induction of the La protein increases. Second, HCV induces La protein. Because the expression of PTB and eIF3 was not significantly induced in the tissue lesions of chronic hepatitis C patients in this study, there must be unknown mechanisms by which HCV infection induces La protein. Our preliminary results showed that HCV proteins increased La protein in Huh-7 cells (data not shown). Further analysis is needed to show the interaction between La protein induction and HCV replication in chronic hepatitis C.

In conclusion, we discovered host factors that regulate HCV translation and replication in the liver. The implication of these findings with regard to the HCV life cycle is shown in Figure 11. Hepatitis and the resulting increased regeneration of hepatocytes increase IRES activity and enhance HCV replication. This may be an important mechanism by which HCV maintains its viral load under host defense immune pressure. These findings shed new light on the mechanism of HCV replication and could be the basis for developing a novel antiviral therapy. Although La protein and PTB have been shown to be involved in the cell-cycle regulation of HCV IRES activity, many other host factors might also be involved.

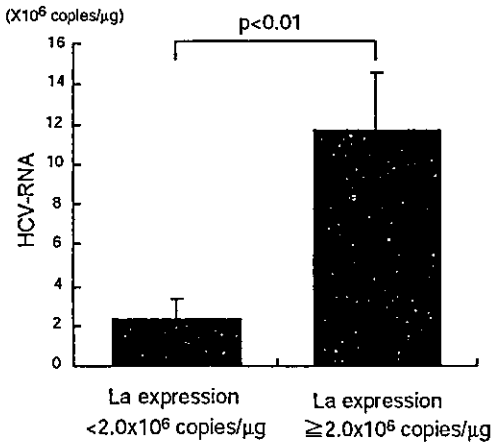

Figure 10. La protein expression and HCV RNA in liver.

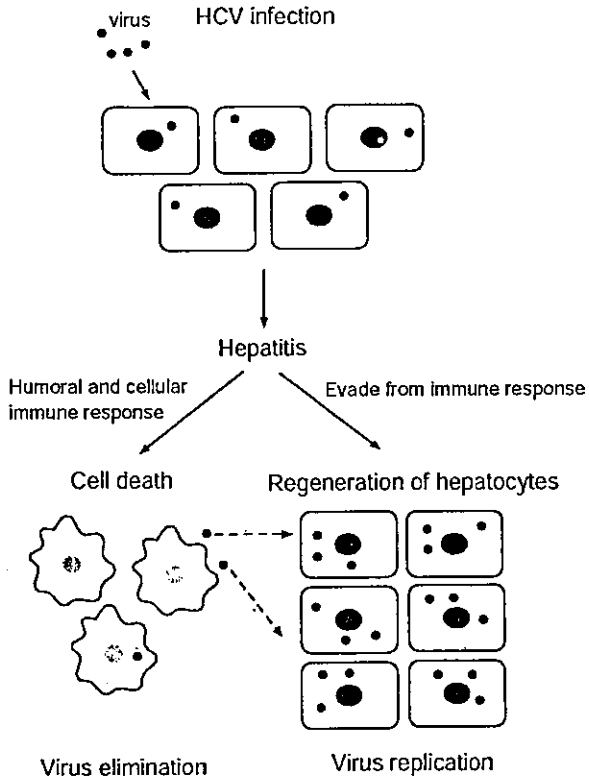

Figure 11. Hepatitis and HCV life cycle.

We are extending these analyses to other initiation factors and investigating the functional role on HCV IRES activity and replication of HCV.

References

1. Choo QL, Kuo G, Weiner AJ, Overby LR, Bradley DW, Houghton M. Isolation of a cDNA clone derived from a blood-borne non-A, non-B viral hepatitis genome. Science 1989;244:359–362.
2. Kiyosawa K, Sodeyama T, Tanaka E, Gibo Y, Yoshizawa K, Nakano Y, Furuta S, Akahane Y, Nishioka K, Purcell RH, et al. Interrelationship of blood transfusion, non-A, non-B hepatitis and hepatocellular carcinoma: analysis by detection of antibody to hepatitis C virus. Hepatology 1990;12:671–675.
3. Davies MV, Pelletier J, Meerovitch K, Sonenberg N, Kaufman RJ. The effect of poliovirus proteinase 2Apro expression on cellular metabolism. Inhibition of DNA replication, RNA polymerase II transcription, and translation. J Biol Chem 1991;266: 14714–14720.
4. McHutchison JG, Gordon SC, Schiff ER, Shiffman ML, Lee WM, Rustgi VK, Goodman ZD, Ling MH, Cort S, Albrecht JK. Interferon alfa-2b alone or in combination with ribavirin as initial treatment for chronic hepatitis C. Hepatitis Interventional Therapy Group. N Engl J Med 1998;339:1485–1492.
5. Poynard T, Marcellin P, Lee SS, Niederau C, Minuk GS, Ideo G, Bain V, Heathcote J, Zeuzem S, Trepo C, Albrecht J. Randomised trial of interferon alpha2b plus ribavirin for 48 weeks or for 24 weeks versus interferon alpha2b plus placebo for 48 weeks for treatment of chronic infection with hepatitis C virus. International Hepatitis Interventional Therapy Group (IHIT). Lancet 1998;352:1426–1432.
6. Fried MW, Shiffman ML, Reddy KR, Smith C, Marinos G, Goncales FL Jr, Haussinger D, Diago M, Carosi G, Dhumeaux D, Craxi A, Lin A, Hoffman J, Yu J. Peginterferon alfa-2a plus ribavirin for chronic hepatitis C virus infection. N Engl J Med 2002;347:975–982.
7. Pestova TV, Shatsky IN, Fletcher SP, Jackson RJ, Hellen CU. A prokaryotic-like mode of cytoplasmic eukaryotic ribosome binding to the initiation codon during internal translation initiation of hepatitis C and classical swine fever virus RNAs. Genes Dev 1998;12:67–83.
8. Wang C, Sarnow P, Siddiqui A. Translation of human hepatitis C virus RNA in cultured cells is mediated by an internal ribosome-binding mechanism. J Virol 1993;67:3338–3344.
9. Reynolds JE, Kaminski A, Kettinen HJ, Grace K, Clarke BE, Carroll AR, Rowlands DJ, Jackson RJ. Unique features of internal initiation of hepatitis C virus RNA translation. EMBO J 1995;14:6010–6020.
10. Lu HH, Wimmer E. Poliovirus chimeras replicating under the translational control of genetic elements of hepatitis C virus reveal unusual properties of the internal ribosomal entry site of hepatitis C virus. Proc Natl Acad Sci U S A 1996;93:1412–1417.
11. Honda M, Ping LH, Rijnbrand RC, Amphlett E, Clarke B, Rowlands D, Lemon SM. Structural requirements for initiation of translation by internal ribosome entry within genome-length hepatitis C virus RNA. Virology 1996;222:31–42.
12. Wang C, Sarnow P, Siddiqui A. A conserved helical element is essential for internal initiation of translation of hepatitis C virus RNA. J Virol 1994;68:7301–7307.
13. Rijnbrand RC, Abbink TE, Haasnoot PC, Spaan WJ, Bredenbeek PJ. The influence of AUG codons in the hepatitis C virus 5′ nontranslated region on translation and mapping of the translation initiation window. Virology 1996;226:47–56.
14. Honda M, Brown EA, Lemon SM. Stability of a stem-loop involving the initiator AUG controls the efficiency of internal initiation of translation on hepatitis C virus RNA. RNA 1996;2:955–968.
15. Honda M, Beard MR, Ping LH, Lemon SM. A phylogenetically conserved stem-loop structure at the 5′ border of the internal ribosome entry site of hepatitis C virus is required for cap-independent viral translation. J Virol 1999;73:1165–1174.
16. Ali N, Siddiqui A. The La antigen binds 5′ noncoding region of the hepatitis C virus RNA in the context of the initiator AUG codon and stimulates internal ribosome entry site-mediated translation. Proc Natl Acad Sci U S A 1997;94:2249–2254.
17. Ali N, Pruijn GJ, Kenan DJ, Keene JD, Siddiqui A. Human La antigen is required for the hepatitis C virus internal ribosome entry site-mediated translation. J Biol Chem 2000;275:27531–27540.
18. Ali N, Siddiqui A. Interaction of polypyrimidine tract-binding protein with the 5′ noncoding region of the hepatitis C virus RNA genome and its functional requirement in internal initiation of translation. J Virol 1995;69:6367–6375.
19. Chung RT, Kaplan LM. Heterogeneous nuclear ribonucleoprotein I (hnRNP-I/PTB) selectively binds the conserved 3′ terminus of hepatitis C viral RNA. Biochem Biophys Res Commun 1999;254: 351–362.
20. Spangberg K, Schwartz S. Poly(C)-binding protein interacts with the hepatitis C virus 5′ untranslated region. J Gen Virol 1999; 80:1371–1376.
21. Sachs AB. Cell cycle-dependent translation initiation: IRES elements prevail. Cell 2000;101:243–245.
22. Honda M, Kaneko S, Matsushita E, Kobayashi K, Abell GA, Lemon SM. Cell cycle regulation of hepatitis C virus internal ribosomal entry site-directed translation. Gastroenterology 2000; 118:152–162.
23. Shimazaki T, Honda M, Kaneko S, Kobayashi K. Inhibition of internal ribosomal entry site-directed translation of HCV by re-

combinant IFN-alpha correlates with a reduced La protein. Hepatology 2002;35:199–208.
24. Gosert R, Chang KH, Rijnbrand R, Yi M, Sangar DV, Lemon SM. Transient expression of cellular polypyrimidine-tract binding protein stimulates cap-independent translation directed by both picornaviral and flaviviral internal ribosome entry sites in vivo. Mol Cell Biol 2000;20:1583–1595.
25. Siomi MC, Eder PS, Kataoka N, Wan L, Liu Q, Dreyfuss G. Transportin-mediated nuclear import of heterogeneous nuclear RNP proteins. J Cell Biol 1997;138:1181–1192.
26. Wang X, Liebhaber SA. Complementary change in cis determinants and trans factors in the evolution of an mRNP stability complex. EMBO J 1996;15:5040–5051.
27. Gaspar NJ, Kinzy TG, Scherer BJ, Humbelin M, Hershey JW, Merrick WC. Translation initiation factor eIF-2. Cloning and expression of the human cDNA encoding the gamma-subunit. J Biol Chem 1994;269:3415–3422.
28. Johnson KR, Merrick WC, Zoll WL, Zhu Y. Identification of cDNA clones for the large subunit of eukaryotic translation initiation factor 3. Comparison of homologues from human, *Nicotiana tabacum*, *Caenorhabditis elegans*, and *Saccharomyces cerevisiae*. J Biol Chem 1997;272:7106–7113.
29. Hanecak R, Brown-Driver V, Fox MC, Azad RF, Furusako S, Nozaki C, Ford C, Sasmor H, Anderson KP. Antisense oligonucleotide inhibition of hepatitis C virus gene expression in transformed hepatocytes. J Virol 1996;70:5203–5212.
30. Honda M, Kaneko S, Kawai H, Shirota Y, Kobayashi K. Differential gene expression between chronic hepatitis B and C hepatic lesion. Gastroenterology 2001;120:955–966.
31. Kruger M, Beger C, Li QX, Welch PJ, Tritz R, Leavitt M, Barber JR, Wong-Staal F. Identification of eIF2Bgamma and eIF2gamma as cofactors of hepatitis C virus internal ribosome entry site-mediated translation using a functional genomics approach. Proc Natl Acad Sci U S A 2000;97:8566–8571.
32. Buratti E, Tisminetzky S, Zotti M, Baralle FE. Functional analysis of the interaction between HCV 5'UTR and putative subunits of eukaryotic translation initiation factor eIF3. Nucleic Acids Res 1998;26:3179–3187.
33. Michel YM, Borman AM, Paulous S, Kean KM. Eukaryotic initiation factor 4G-poly(A) binding protein interaction is required for poly(A) tail-mediated stimulation of picornavirus internal ribosome entry segment-driven translation but not for X-mediated stimulation of hepatitis C virus translation. Mol Cell Biol 2001;21:4097–4109.
34. Cornelis S, Bruynooghe Y, Denecker G, Van Huffel S, Tinton S, Beyaert R. Identification and characterization of a novel cell cycle-regulated internal ribosome entry site. Mol Cell 2000;5:597–605.
35. Sachs AB, Sarnow P, Hentze MW. Starting at the beginning, middle, and end: translation initiation in eukaryotes. Cell 1997;89:831–838.
36. Kawai HF, Kaneko S, Honda M, Shirota Y, Kobayashi K. Alpha-fetoprotein-producing hepatoma cell lines share common expression profiles of genes in various categories demonstrated by cDNA microarray analysis. Hepatology 2001;33:676–691.
37. Shirota Y, Kaneko S, Honda M, Kawai HF, Kobayashi K. Identification of differentially expressed genes in hepatocellular carcinoma with cDNA microarrays. Hepatology 2001;33:832–840.
38. Takeuchi T, Katsume A, Tanaka T, Abe A, Inoue K, Tsukiyama-Kohara K, Kawaguchi R, Tanaka S, Kohara M. Real-time detection system for quantification of hepatitis C virus genome. Gastroenterology 1999;116:636–642.
39. Pestova TV, Kolupaeva VG, Lomakin IB, Pilipenko EV, Shatsky IN, Agol VI, Hellen CU. Molecular mechanisms of translation initiation in eukaryotes. Proc Natl Acad Sci U S A 2001;98:7029–7036.
40. Pflugheber J, Fredericksen B, Sumpter R Jr, Wang C, Ware F, Sodora DL, Gale M Jr. Regulation of PKR and IRF-1 during hepatitis C virus RNA replication. Proc Natl Acad Sci U S A 2002;99:7029–7036.

Received March 16, 2004. Accepted November 4, 2004.

Address requests for reprints to: Shuichi Kaneko, MD, PhD, Department of Gastroenterology, Graduate School of Medicine, Kanazawa University, Takara-Machi 13-1, Kanazawa, 920-8641, Japan. e-mail: skaneko@medf.m.kanazawa-u.ac.jp; fax: (81) 76-234-4250.

The authors thank Masami Ueda, Junko Hara, and Mikiko Nakamura for excellent technical assistance.